Available online at www.sciencedirect.com
SCIENCE DIRECT®
Sensors and Actuators B xxx (2004) xxx–xxx
SENSORS AND ACTUATORS B CHEMICAL
www.elsevier.com/locate/snb

Gas-sensitive properties of thin and thick film sensors based on Fe_2O_3–SnO_2 nanocomposites

D. Kotsikau [a,*], M. Ivanovskaya [a], D. Orlik [a], M. Falasconi [b]

[a] Scientific Research Institute for Physical and Chemical Problems, Belarus State University, Leningradskaya 14, 220050 Minsk, Belarus
[b] INFM-Gas Sensor Laboratory, University of Brescia, Via Valotti 9, 25133 Brescia, Italy

Received 15 December 2003; received in revised form 10 February 2004; accepted 18 February 2004

Abstract

Influence of phase composition, structural peculiarities and grain size of Fe_2O_3–SnO_2 nanocomposites prepared by sol–gel technology on gas-sensitive properties of the corresponding gas sensors has been studied in the paper. The characteristics of thin film sensors were obtained with regards to NO_2 and C_2H_5OH. Behaviour of thick film sensors was estimated in humid C_2H_5OH ambient. High sensitivity of Fe_2O_3–SnO_2 samples containing highly dispersive Fe_2O_3 phase has been revealed. The composites consisting of poorly crystallised α-Fe_2O_3 along with Sn(IV)–α-Fe_2O_3 solid solution demonstrate maximum sensitivity to ethanol. Structural and functional distinctions of the Fe_2O_3–SnO_2 composites obtained by using different Fe-precursors (Fe^{3+} and Fe^{2+} inorganic salts) have been revealed. Mechanisms of the processes, which determine gas-sensitive behaviour of the composites, are considered.

Keywords: Fe_2O_3–SnO_2 nanocomposites; Structural characteristics; Gas sensitivity

1. Introduction

SnO_2-based composites are commonly used materials for gas sensing application. Simple SnO_2 is characterised by low sensitivity and unsuitable selectivity to most of toxic and explosive gases [1–3]. This objective causes the necessity of SnO_2 modifying by various additives like noble metals (Pd, Pt, Au) [4] and metal ions of variable valency (Mo, Ni, Fe, Sb). One of the most prospective ways to achieve good sensor performance is the obtaining sensitive layers of complex composition, where the functions of receptor and transducer are divided between different phases [5]. As it has been established by Yamazoe [6], metal cations, which are characterised by electronegativity lower than electronegativity of Sn(IV), increase the sensitivity of SnO_2-based sensors to ethanol.

The analysis of the existing literature shows that the layers based on the Fe_2O_3–SnO_2 composites possess high sensitivity to ethanol and suitable response to NO_2, CO and CH_4.

Tan et al. [7] reported good ethanol sensitivity values of Fe_2O_3–SnO_2 thick film as high as 850 at 1000 ppm in air. The sensor is selective to ethanol over carbon monoxide and hydrogen. The functional parameters are also found to be very stable.

The introduction of Fe in SnO_2 thin films by means of RGTO technique leads to the formation of the new ternary compound $Sn_xFe_{1-x}O_y$, which shows high response to CO [8]. Maximum sensitivity (3. 2 for 500 ppm) was observed for Fe content of 1. 8%.

Suitable low-temperature detection of CH_4 by α-Fe_2O_3 (SO_4^{2-}, Sn) thick films as compared to other metal oxides was achieved by Chung and Lee [9]. As it was found, α-Fe_2O_3 (SO_4^{2-}, Sn) powders precipitated at different pH values exhibited different microstructures.

Remarkably, that structural peculiarities of oxide materials such as phase composition, dispersity and morphology, influence strongly the functional features (sensitivity, selectivity, long-term stability) of the corresponding gas sensors [1,10]. Moreover, type of sensitive layer (ceramic, thin film, thick film) determines substantially a sensor performance as well. But the fine structural features of an oxide system and its activity in reduction–oxidation reactions are not commonly taking into consideration.

This paper reports an investigation on structural and functional features of the Fe_2O_3–SnO_2 composites prepared by different variations of the sol–gel technology. An attempt to establish correlation between the fine structural peculiarities

* Corresponding author. Tel.: +375-17-220-81-06; fax: +375-17-226-46-96; mobile: +375-296808106.
E-mail address: kotsikau@bsu. by (D. Kotsikau).

0925-4005/$ – see front matter © 2004 Published by Elsevier B.V.
doi:10.1016/j.snb.2004.02.051

of the complex oxide systems and their gas-sensitive properties regarding NO_2 and C_2H_5OH has been made.

2. Experimental

Simple oxides/hydroxides of iron and tin were prepared by hydrolysis of the corresponding inorganic precursors by using base agent (aqueous solution of NH_3). The precipitate then was washed thoroughly and transformed into colloidal solution (sol). The Fe_2O_3–SnO_2 composites (Fe:Sn = 1:9, 1:1, 9:1) were formed by mixing iron and tin oxides/hydroxides in the required proportions followed by annealing of the dried species at different temperatures (300, 500, 600, 800 °C) [5]. Fe^{2+} precursors ($FeCl_2$, $FeSO_4$) were used along with more common Fe^{3+} inorganic salts ($FeCl_3$, $Fe(NO_3)_3$, $Fe_2(SO_4)_3$. Using Fe^{3+} precursors leads to the formation of α-Fe_2O_3 species; meanwhile, hydrolysis of Fe^{2+} salts under certain conditions allows to obtain metastable γ-modification of iron oxide [10]. Thus, two types of the composites were prepared: α-Fe_2O_3–SnO_2 (by mixing α-Fe_2O_3 and SnO_2 sols) and γ-Fe_2O_3–SnO_2 (by mixing γ-Fe_2O_3 and SnO_2 sols).

Structural investigations were carried out by XRD, EPR, TEM and Mössbauer spectroscopy.

The sensing layers were heated at 550 °C in air during 20 h. High-temperature treatment provides measurable range of the layer resistance. Measurements of the temperature-dependent conductivity of the oxide layers were carried out in the region of temperature 100–500 °C at RH 30%. Gas-sensitive properties of thin film species were mostly studied regarding 1 ppm NO_2 (RH 40%). Thick film sensors were measured in humid ethanol vapours (RH 98%) within the range 0. 025–1. 0‰ (0. 1‰ corresponds to 45 mg/m^3 of ethanol), thus modelling alcohol content in human's expirated air. A flow of gas was obtained by commercial ethanol generator GS-1 (Analitpribor, Kiev). The construction of the sensors is described elsewhere [11]. The sensor response was calculated as $(I_{gas} - I_{air})/I_{air}$ at fixed U-value for thin films and as $(R_{gas} - R_{air})/R_{air}$ in the case of thick film layers at detection of reducing gases and as $(I_{air} - I_{gas})/I_{gas}$ and $(R_{air} - R_{gas})/R_{gas}$ when detecting oxidising ambient, correspondingly; where I_{gas} and R_{gas} are current and layer conductivity in gas ambient; I_{air} and R_{air} are current and layer conductivity in air.

3. Results and discussion

The Fe_2O_3–SnO_2 composites of the same Fe:Sn ratio prepared via Fe^{2+} and Fe^{3+} precursors differ considerably regarding their phase composition (Fig. 1a and b). The sharpest distinctions are observed when the samples been heated at temperatures below 500 °C. It is important to note, that all the oxide systems mentioned in this paper are characterised by high system dispersity and relatively low degree of crystallinity (Table 1). The grain size of the samples annealed at 500 °C does not exceed 6 nm.

The XRD reflections assigned to the α-Fe_2O_3–SnO_2 composites within the whole series of the applied component ratios (Fe:Sn = 9:1, 1:1, 1:9) appear to be broad and low-intensive. This can be explained by very small size of SnO_2 grains (about 2 nm) and poor crystallinity of α-Fe_2O_3 phase. The composites with Fe:Sn ratio 1:9 and 1:1 have the structure of Fe(III)–SnO_2 solid solution; in the case of the Fe_2O_3–SnO_2 (Fe:Sn 9:1), Sn(IV)–α-Fe_2O_3 solid solution is typical.

Fast removal of water and crystallisation of α-Fe_2O_3 occur at temperatures above 500 °C: the reflections of this phase become narrow. Noticeable SnO_2 particle agglomeration accompanying the crystallisation processes was only observed at 800 °C. High-temperature treatment results in partial decomposition of the sample structure and isolation of simple oxide phases—SnO_2 and α-Fe_2O_3; the samples become heterogeneous.

As opposed to α-Fe_2O_3, γ-Fe_2O_3 phase obtained by using the mentioned synthesis technique after drying at 150 °C is characterised by rather well crystallinity and absence of constitutional water. However, annealing the sample based on metastable γ-Fe_2O_3 phase at 400–500 °C results in its transforming into α-Fe_2O_3 one. Thus, the XRD patterns of both α-Fe_2O_3–SnO_2 and γ-Fe_2O_3–SnO_2 species of the same component ratio become similar after heating at 800 °C. Besides, according to Mössbauer study, small areas of amorphous and highly dispersive Fe_2O_3 phase are also preserved within the α-Fe_2O_3–SnO_2 and γ-Fe_2O_3–SnO_2 (Fe:Sn = 9:1, 1:1) samples up to 400 °C. EPR and Mössbauer studies give evidence that the α-Fe_2O_3 phase obtained through the amorphous Fe_2O_3 (via Fe^{3+} precursor) and by the thermally stimulated transformation of γ-Fe_2O_3 (via Fe^{2+} precursor) are significantly different: the motive of γ-Fe_2O_3 structure (cubic symmetry) preserves within the latter species [5]. This phenomenon is also typical of highly dispersive α-modifications of iron oxides/hydroxides (trigonal symmetry). Note, that in the case of the γ-Fe_2O_3–SnO_2 composites the grain size of both oxide phases (Fe_2O_3 and SnO_2) is greater as compared to the α-Fe_2O_3–SnO_2. This effect is typical of all series of component ratios and annealing temperatures. Consequently, one can expect that the samples based on γ-Fe_2O_3 and α-Fe_2O_3 will demonstrate different gas-sensitive behaviour.

3.1. Electrical measurements in air

Electrical conductivity of the Fe_2O_3–SnO_2 thin film layers with Fe:Sn = 1:9 and 1:1 is found to be considerably lower as compared to the Fe_2O_3–SnO_2 (Fe:Sn = 9:1) composite and simple oxides in air (Fig. 2). The Fe_2O_3–SnO_2 (Fe:Sn = 9:1) and SnO_2 demonstrate minimum resistance values. The conductivity of the Fe_2O_3–SnO_2 (Fe:Sn = 1:9, 1:1) films is approximately equal at 100–500 °C; however, the trends of the curves are quite dissimilar within the indi-

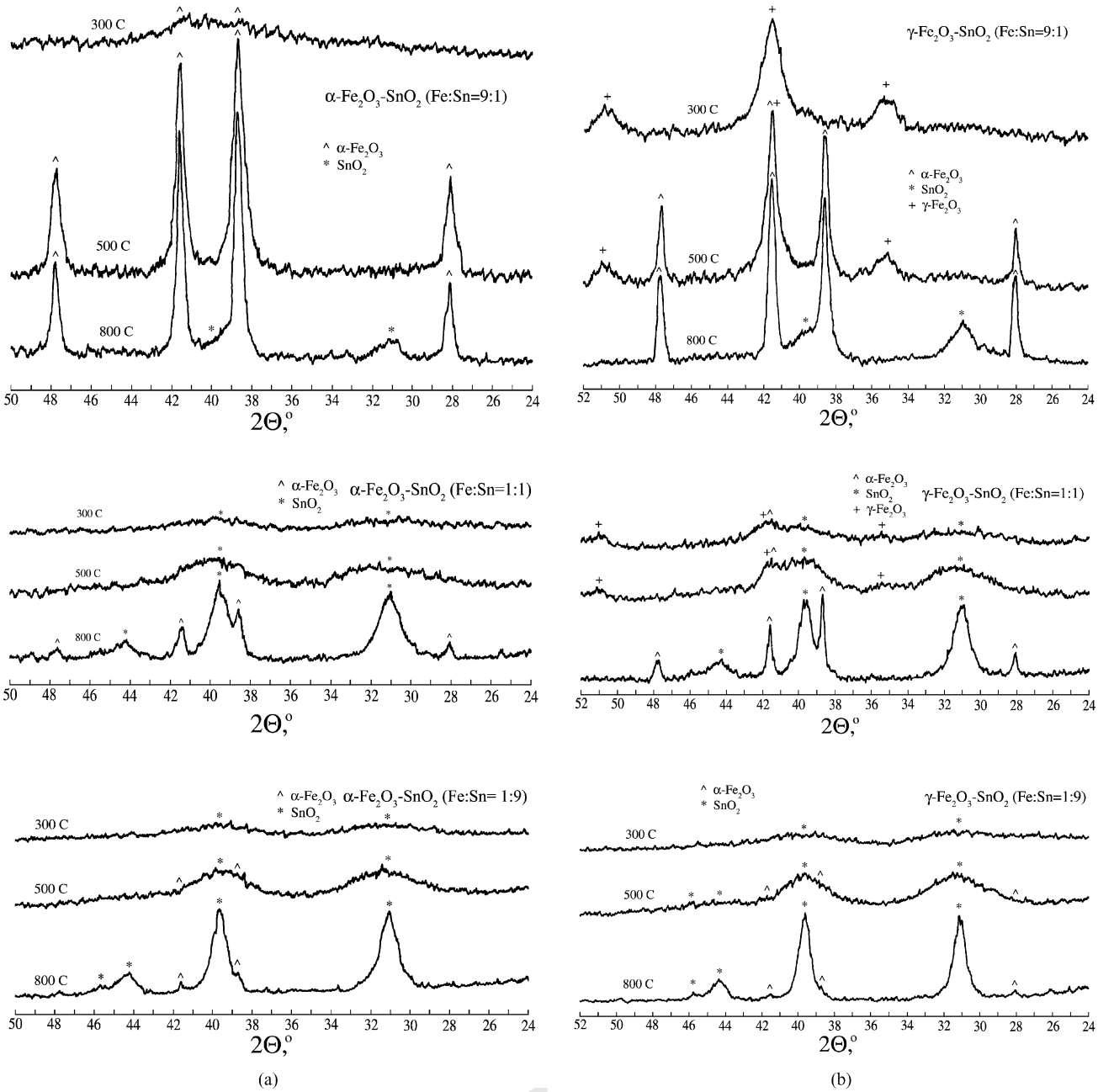

Fig. 1. XRD patterns of α-Fe_2O_3–SnO_2 (a) and γ-Fe_2O_3–SnO_2 (b) composites (Fe:Sn = 9:1, 1:1, 1:9), annealed at different temperatures for 1 h.

Table 1
Phase composition and grain size of simple Fe_2O_3 and SnO_2 oxides and Fe_2O_3–SnO_2 nanocomposites depending on annealing temperature

T (°C)	SnO_2 d (nm)	Fe_2O_3 d (nm)	α-Fe_2O_3–SnO_2 (Fe:Sn = 1:1)		γ-Fe_2O_3–SnO_2 (Fe:Sn = 1:1)	
			Phase	d (nm)	Phase	d (nm)
300	2	–	SnO_2	2	SnO_2	2
			α-Fe_2O_3	2	γ-Fe_2O_3	4
500	6	15	SnO_2	3	SnO_2	5
			α-Fe_2O_3	3	(α + γ)-Fe_2O_3	6
800	40	70	SnO_2	10	SnO_2	10
			α-Fe_2O_3	30	α-Fe_2O_3	45

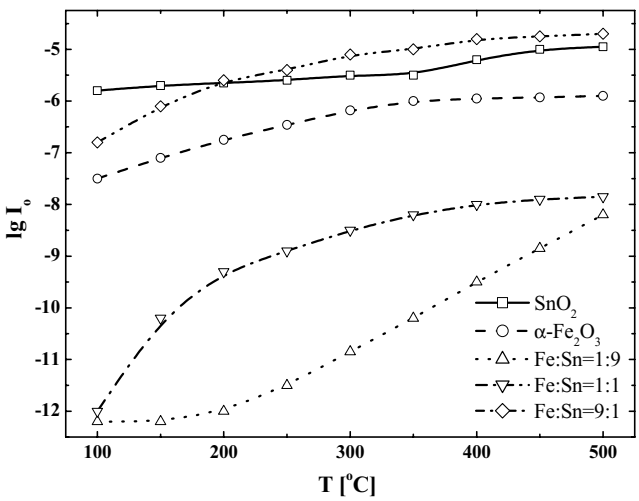

Fig. 2. Temperature-dependent conductivity of thin film simple oxides and α-Fe_2O_3–SnO_2 composites in air, RH 30%.

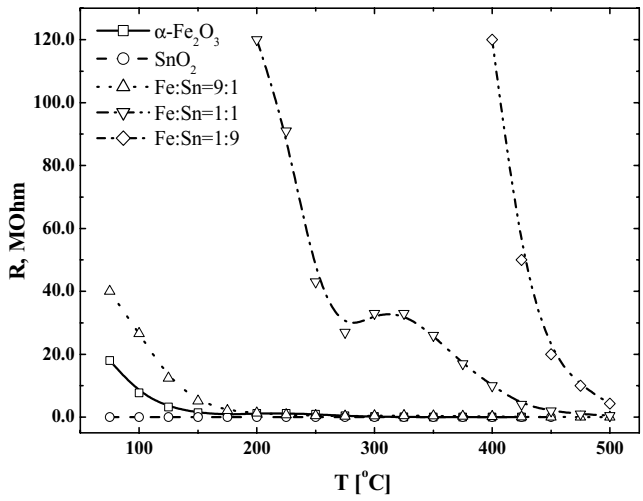

Fig. 3. Temperature-dependent resistance of thick film simple oxides and Fe_2O_3–SnO_2 composites in air, RH 30%.

cated temperature region. In the case of Fe:Sn = 1:9 the conductivity begins to rise gradually starting from 200 °C; the sample with equal content of the components demonstrates maximum conductivity change within a low-temperature region (100–200 °C). The conductivity of SnO_2 is mainly determined by the presence of singly charged oxygen vacancies (V_o^-) [12,13]. Fe^{3+} ions, which occupy the Sn(IV) positions within SnO_2 crystal lattice, are acting as electron acceptors; it results in decrease of charge carrier amount. Meanwhile, [Fe^{3+}–V_o^-] associates are not participating in charge transfer. Temperature increase up to 400–550 °C is an important requirement to provide electron activation and sufficient resistance drop. As it was noted above, the Fe_2O_3–SnO_2 composites consist of highly dispersive oxide phases of iron and tin. The indicated phases are characterised by elevated activity and react readily under heating. Sn–OH–Fe and Sn–O–Fe bonding is possible at SnO_2/Fe_2O_3 phase interface that leads to decreasing the contact resistance and increasing the potential barrier transmissivity.

Surface conductivity mainly contributes to the total conductivity of the thin oxide films at direct current measurements. The surface layer of amorphous Fe_2O_3 doped with Sn^{4+} ions provides an increased conductivity of the Fe_2O_3–SnO_2 (Sn:Fe = 1:1) film as contrast to the Fe_2O_3–SnO_2 (Fe:Sn = 1:9) [14,15]. Adding SnO_2 to Fe_2O_3 brings to increasing the free charge carrier concentration, and consequently, to heightening the conductivity of the Fe_2O_3–SnO_2 (Fe:Sn = 9:1) having the structure of Sn(IV)–α-Fe_2O_3 solid solution.

The thick film layers based on the Fe_2O_3–SnO_2 composites and simple oxides demonstrate the same regularities that intrinsic to the corresponding thin films, but absolute conductivity values appear to be significantly lower in the case of the thick films (Fig. 3). It is probably explained by poor contact between separate particles of the powder. Because of the indicated point we were not able to perform the functional characterisation of some samples at low operating temperatures in both air and gas ambient. The sample with Fe:Sn ratio 1:9 appeared to be of extremely high resistance in air.

3.2. Electrical measurements in gas ambient

Thin and thick Fe_2O_3–SnO_2 films of different structure and chemical composition are characterised by dissimilar behaviour in gas ambient of different chemical nature—oxidising (NO_2) and reducing (C_2H_5OH) gases. Humid ethanol vapours (RH 98%) were used that caused by great importance of control the alcohol concentration in human's expirations. It is obvious, that great humidity influences strongly the sensitive layer behaviour. As it was established by Kappler et al. [16], humidity growth leads to an increase in the number of oxygen vacancies that enhances the chemisorption of oxygen and forms specific oxygen sites. In synthetic air an increase of oxygen ions occurs at the sensor surface when humidity is increased. The rise in the number of available oxygen partners for ethanol in the oxidation reaction causes enhancement of the sensor signal.

The thin film sensors are found to be more suitable for detection of NO_2; meanwhile, the thick films demonstrate good performance when detecting ethanol vapours. Note, that the response values (dG/G) to oxidising gases of all the sensors are very low as compared to individual oxides like SnO_2 and In_2O_3. The response of the best material to 1 ppm NO_2 does not exceed 0. 5 r. u. At lower NO_2 concentration the signal is unstable and poorly reproducible (Fig. 4). The only α-Fe_2O_3–SnO_2 samples show measurable response values to NO_2 among the thin film layers. The α-Fe_2O_3–SnO_2 (Fe:Sn = 1:1) composite demonstrates maximum sensitivity at 100 °C. It is important, that NO_2 molecules proceed as electron donors within low-temperature region. It can be connected with the point that the conductivity of

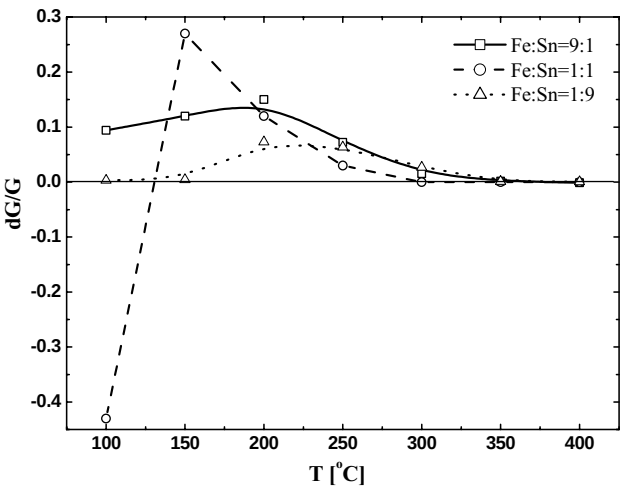

Fig. 4. Temperature dependent response of Fe_2O_3–SnO_2 thin film sensors to 1 ppm NO_2, RH 40%.

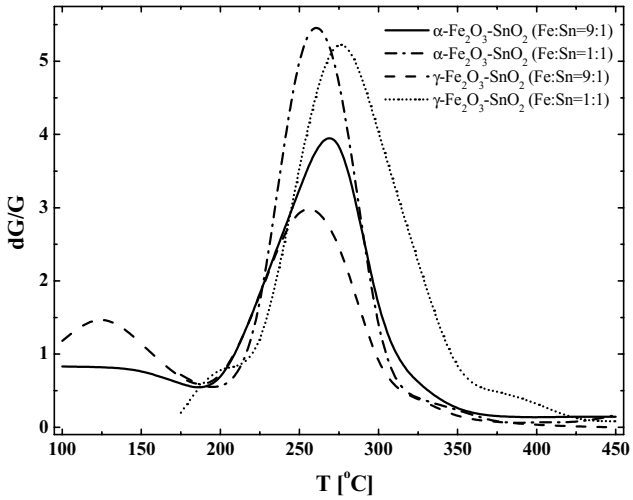

Fig. 5. Temperature-dependent response of α-Fe_2O_3–SnO_2 and γ-Fe_2O_3–SnO_2 thick film sensors to 0. 05‰ of C_2H_5OH.

the Fe_2O_3–SnO_2 composites (up to 150 °C) is determined by the presence of surface OH-groups, which desorbs at 150–400 °C. Besides, the response of the α-Fe_2O_3–SnO_2 sensors of all series of compositions to NO_2 reaches its maximum value at temperatures, at which maximum layer conductivity drop in air is observed.

In the case of thick films, the α-Fe_2O_3–SnO_2 and γ-Fe_2O_3–SnO_2 (Fe:Sn = 9:1) composites show maximum sensitivity to humid C_2H_5OH vapours. As it was noted above, the layers were annealed at 550 °C in order to provide measurable sensor conductivity. Thus prepared samples have the structure of Sn(IV)–α-Fe_2O_3 solid solution, γ-Fe_2O_3 transforms completely into α-Fe_2O_3. However, certain insignificant differences are observed in the α-Fe_2O_3–SnO_2 and γ-Fe_2O_3–SnO_2 behaviour that can be caused by certain distinctions in grain size and microstructure of the samples. Thus, the composites obtained via Fe^{3+} precursor (α-Fe_2O_3–SnO_2) are characterised by higher response and increased optimal detecting temperature (Fig. 5).

Maximum response to ethanol of the Fe_2O_3–SnO_2 (Fe:Sn = 9:1, 1:1) layer appears to be greater than that one demonstrated by simple oxides (SnO_2, Fe_2O_3) (Fig. 6). We failed to measure the Fe_2O_3–SnO_2 (Fe:Sn = 1:9) sensor because of its extremely high resistance. Remarkably, that the optimal operating temperatures of the whole series of the thick film sensors lie in narrow-temperature range (280–320 °C).

The dependence of the thick film sensor resistance vs. concentration of humid ethanol vapour (270 °C) is presented in Fig. 7 . There is a clear difference in the behaviour of the α-Fe_2O_3–SnO_2 and γ-Fe_2O_3–SnO_2 species. The α-Fe_2O_3–SnO_2 layers demonstrate suitable performance when detecting alcohol within the concentration range 0. 05–1. 0‰. In contrast, the γ-Fe_2O_3–SnO_2 composites and simple oxides are characterised by unsuitably low $\Delta R_{layer}/\Delta C_{gas}$ ratio that makes the mentioned materials unusable for accurate registration of the gas concentration.

According to the available EPR data, two types of Fe(III) centres occur within the Fe_2O_3–SnO_2 composites obtained both via Fe^{3+} and Fe^{2+} precursors (Fig. 8): (I) $g = 4.3$, $\Delta B = 4$ mT and (II) $g = 4.3$, $\Delta B = 4$ mT. The signal I, which is observed in the case of SnO_2 doped with Fe^{3+} ions is assigned to isolated Fe(III) centres in strong crystal field of rhombic symmetry [17]. Strong crystal field can be caused by the distribution of Fe(III) ions within near-surface layers of SnO_2, as well as by the presence of oxygen vacancies in close environment of Fe(III) within SnO_2 matrix [18]. Both intensity and shape of the signal II ($g \sim 2.0$) depend on the recording temperature. The spectrum recorded at 77 K allows realising that the broadened resonance signal II contains two lines at $g \sim 2.3$ and ∼2. 0. The former

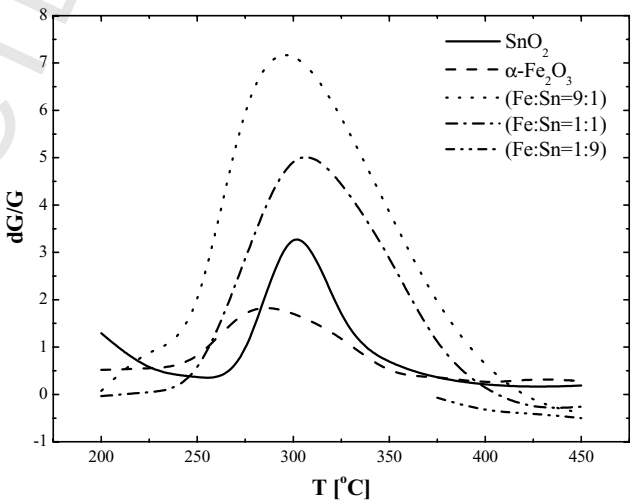

Fig. 6. Temperature-dependent response of thick film sensors based on simple oxides and α-Fe_2O_3–SnO_2 composites to 0. 05‰ of C_2H_5OH.

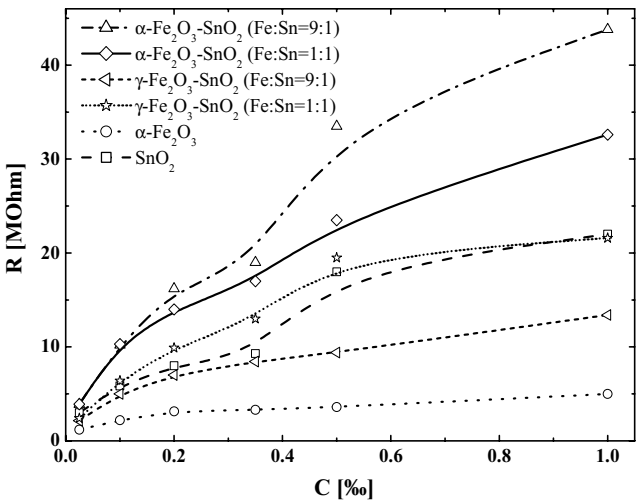

Fig. 7. Concentration-dependent resistance of thick film sensors in humid (RH 98%) C_2H_5OH ambient. Operating temperature 275 °C.

line is assigned to noncrystalline Fe_2O_3 nanoparticles, which consist of Fe(III) ions in cubic symmetry of oxygen close environment. Note, that the mentioned environment is similar to a greater extent to γ-Fe_2O_3/γ-FeOOH crystal structure (cubic symmetry) rather than to trigonal α-Fe_2O_3. The second component of the signal II ($g \sim 2.0$) is assigned to the associates of Fe(III) ions; it is typical of superparamagnetic Fe_2O_3 clusters. This fact explains activity of the studied species in gas adsorption processes. Thus, gas-sensitive and electro-physical properties of the thin and thick film Fe_2O_3–SnO_2 are substantially determined by Fe(III) state.

Treating the Fe_2O_3–SnO_2 (Fe:Sn = 1:1) powder with NO_2 (120 °C, 10 min) leads to the increase of the signal II only; the signal I remains unchanged. This fact gives evidence that only amorphous Fe_2O_3 can participate in NO_2 adsorption; the isolated Fe(III) ions within SnO_2 lattice are inactive. This explains greater sensitivity of the Fe_2O_3–SnO_2 (Fe:Sn = 1:1 and 9:1) films to NO_2 as compared to Fe_2O_3–SnO_2 (Fe:Sn = 1:9).

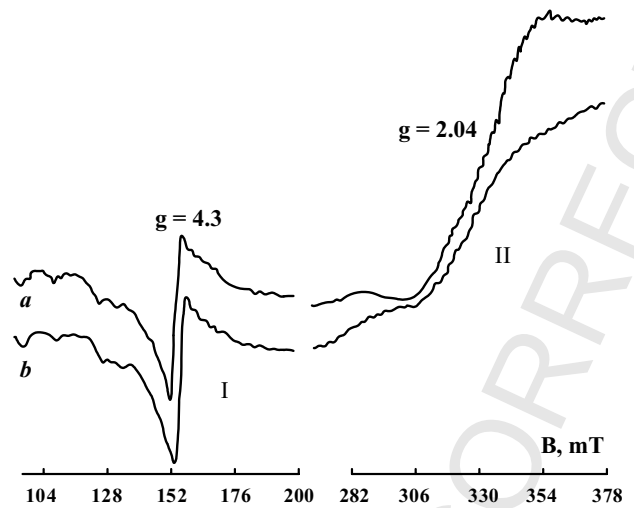

Fig. 8. EPR spectrum of Fe_2O_3–SnO_2 (Fe:Sn = 1:1) powder: (a) initial; (b) treated with NO_2 (10 min, 130 °C).

Table 2
Parameters of ^{57}Fe Mössbauer spectra of Fe_2O_3 and Fe_2O_3–SnO_2 composite

Sample	δ (mm/s)	Δ (mm/s)	B (T)
Fe_2O_3–SnO_2 (Fe:Sn 1:1), 300 °C	0. 35 ± 0. 02	0. 72 ± 0. 02	50. 8
Fe_2O_3–SnO_2 (Fe:Sn 1:1), 500 °C	0. 35 ± 0. 02	0. 87 ± 0. 02	50. 8
γ-Fe_2O_3 (bulk)	0. 34 ± 0. 01	−0. 053 ± 0. 020	49. 6
α-Fe_2O_3 (bulk)	0. 47 ± 0. 03	0. 23 ± 0. 01	51. 8
Fe_2O_3 (amorphous)	0. 39 ± 0. 02	0. 09 ± 0. 01	50. 7

Recorded at 300 K.

Mössbauer spectra of the α-Fe_2O_3–SnO_2 and γ-Fe_2O_3–SnO_2 samples (annealing temperature 300–500 °C) represent a broadened doublet, which is an evidence of superparamagnetic Fe_2O_3 particles ($d \sim 3$–4 nm) formation. Thus, the samples with Fe:Sn = 9:1 and 1:1 contain areas of highly dispersive and poorly crystallised Fe_2O_3. The parameters of the Fe_2O_3–SnO_2 spectra are different from the parameters, which are typical of the spectra of both α-Fe_2O_3 and γ-Fe_2O_3 bulk phases. However, the values of isomeric shift (δ) and induction of magnetic field (B) of amorphous Fe_2O_3 are closer to the parameters of cubic γ-Fe_2O_3 rather than to trigonal α-Fe_2O_3 that is in agreement with the EPR data (Table 2). The coordination of Fe(III), which is specific of cubic structure of unit cell (γ-FeOOH, γ-Fe_2O_3), preserves within the Fe_2O_3 amorphous phase. Considerable increase of the quadrupole splitting (Δ) values as compared to the simple oxides is typical of the studied composites; it indicates that the crystal environment of Fe(III) points within the Fe_2O_3 matrix is strongly irregular in the presence of Sn(IV).

Two ways of alcohol (in particular, ethanol) molecule conversion are possible at oxide surface—dehydrogenation (1) and dehydration (2) [6,19]:

$$CH_3CH_2OH \rightarrow CH_3CHO + \tfrac{1}{2}H_2 \quad \text{(dehydrogenation)} \quad (1)$$

$$CH_3CH_2OH \rightarrow C_2H_4 + H_2O \quad \text{(dehydration)} \quad (2)$$

Besides, further oxidation of the formed products (foremost, oxidation of H atoms) is also possible; it should result in sensor response growth. Thus, the process (1) most often proceeds through the oxidising dehydrogenation mechanism:

$$CH_3CH_2OH \xrightarrow{O^{2-},O^-} CH_3CHO + H_2O$$

$$\text{(oxidising dehydrogenation)} \quad (3)$$

As we established earlier [11], lattice oxygen is only participating in the indicated process at high operating temperatures (300–400 °C). The role of adsorbed oxygen consists of regenerating of partially reduced oxide surface.

The oxidising dehydrogenation is heterolytic catalytic reaction. The process involves both reductive–oxidative and acid–base steps. In particular, alcohol molecule adsorption at metal cations, which play role of Lewis centres, is related to acid–base reaction. The reactivity of oxides in acid–base reactions depends on the electronegativity of cations M^{n+}:

$$\chi = \chi_o(2n + 1) \quad (4)$$

where χ_o is the Pauling's electronegativity, n the ion charge. The electronegativity can be used as the measure of Lewis acid activity [20]. Adsorption of alcohol molecules at Lewis sites is going with great output. The relative measure of an oxide activity in the oxidation reactions can be oxygen–oxide surface bonding energy. Lesser energies of oxygen atom isolation from an oxide surface favour higher oxide oxidising ability. Complete oxidation of the intermediate products is possible at the surface of the oxide, which is characterised by small values of M–O bonding energy and electronegativity. Thus, due to the low Fe–O bonding energy and increased basicity of Fe_2O_3 in comparison to SnO_2 ($E_{Fe–O} = 56$, $E_{Sn–O} = 70$ kcal/g per atom; $\chi(Fe^{2+}) = 13.72$, $\chi(Sn^{4+}) = 17.64$) Fe(III) centres promote further oxidation of intermediate products of ethanol molecule transformation [21]. For the detailed mechanism of ethanol detection refer to [22].

Thus, substitution of Sn(IV) for the isolated Fe(III) ions in points of SnO_2 lattice decreases considerably electrical conductivity of SnO_2 films and their sensitivity to both oxidising (NO_2) and reducing (C_2H_5OH) gases. As it was noted above, the Fe_2O_3–SnO_2 nanocomposites, which have a structure of Sn(IV)–α-Fe_2O_3 solid solution, show high response to ethanol vapours due to the presence of two types of adsorption centres—Sn(IV) and Fe(III). The two centres are characterised by different activity in the course of both reduction–oxidation and acid–base reactions.

Moreover, high dispersity of Sn(IV)–α-Fe_2O_3 solid solution provides efficient electron exchange between the cations: Fe(III) ↔ Fe(II). All this produces greater conductivity drop of the active layer and, consequently, improves the sensor performance.

4. Conclusion

Sol–gel technology provides the obtaining of complex oxide systems, which differ by chemical composition (oxide nature, component ratio), structure (phase composition, peculiarities of microstructure) and dispersity.

As it was found out, the studied composites are characterised by distinct electrical properties in both air and gas ambient. Besides, type of the used sensors (thin and thick film) influences strongly the functional features of the layers as well. The correlation between the indicated factors and gas-sensitive performance of the sensors has been established. Thus, doping SnO_2 with Fe^{3+} ions leads to the sensor response decrease to most of gases, in particular NO_2 and C_2H_5OH, that is caused by the occurrence of separately distributed Fe(III) ions within SnO_2 matrix; no clusters of amorphous Fe_2O_3 are present. Good performance of the sensors is typical of the Fe_2O_3–SnO_2 composites with Fe:Sn ≥ 1. Advanced oxide gas-sensitive materials were obtained under the used conditions of synthesis and mode of thermal treatment of the layers. The highly defective α-Fe_2O_3 phase provides suitable sensor conductivity and high sensitivity. Besides, the occurrence of two types of adsorption centres (Sn(IV) and Fe(III)), which possess different activity in both reduction–oxidation and acid–base reactions results in additional improvement of the sensor sensitivity to ethanol vapours.

Certain distinctions were revealed in the behaviour of the Fe_2O_3–SnO_2 composites obtained either through the crystallisation of amorphous Fe_2O_3 or as a result of thermally induced transformation of γ-Fe_2O_3. The composites obtained via Fe^{2+} precursors differ by slightly decreased response and unsuitable $\Delta R_{layer}/\Delta C_{gas}$ ratio as compared to the corresponding species prepared through the Fe^{3+} salt hydrolysis.

Acknowledgements

This work has been supported by INTAS program (project No. 2000-0066).

References

[1] P.G. Harrison, Chemistry of Tin, Chapman & Hall, New York, 1989, Chapter 12, pp. 413–418.
[2] F.H. Chibirova, E.E. Gutman, Structural defects and gas-sensitive properties of some semiconductor metal oxides, Russ. J. Phys. Chem. 74 (9) (2000) 1555–1561.
[3] D. Orlik, M. Ivanovskaya, A. Gurlo, Properties of ceramic semiconductor sensors based on SnO_2–Sb_2O_3, Russ. J. Anal. Chem. 52 (1) (1997) 69–73.
[4] A. Cabot, A. Dieguez, A. Romano-Rodriguez, et al., Influence of the catalytic introduction procedure on the nano-SnO_2 gas sensor performances, Sens. Actuators B: Chem. 79 (2001) 98–106.
[5] M. Ivanovskaya, D. Kotsikau, G. Faglia, et al., Gas-sensitive properties of thin film heterostructures based on Fe_2O_3–In_2O_3 nanocomposites, Sens. Actuators B: Chem. 93 (2003) 422–430.
[6] N. Yamazoe, New approaches for improving semiconductor gas sensors, Sens. Actuators B: Chem. 5 (1991) 7–19.
[7] O. Tan, W. Zhu, Q. Yan, et al., Size effect and gas sensing characteristics of nanocrystalline $x$$SnO_2$–$(1 - x)$α-$Fe_2O_3$ ethanol sensors, Sens. Actuators B: Chem. 65 (2000) 361–365.
[8] P. Bonzi, L. Depero, F. Parmigiani, et al., Formation and structure of tin–iron oxide thin film CO sensors, Mater. Res. Soc. 9 (5) (1994) 1250–1256.
[9] W. Chung, D. Lee, Characteristics of α-Fe_2O_3 thick film gas sensors, Thin Solid Films 200 (1991) 329–339.
[10] Sh.K. Shaikhutdinov, Y. Joseph, C. Kuhrs, et al., Faraday Discuss. 114 (1999) 363–380.
[11] M. Ivanovskaya, P. Bogdanov, G. Faglia, et al., The features of thin film and ceramic sensors for the detection of CO and NO_2, Sens. Actuators B: Chem. 68 (2000) 344–350.

[12] P.G. Harrison, M.J. Willett, Tin oxide surfaces, J. Chem. Soc., Faraday Trans. 1 85 (8) (1989) 1921–1932.
[13] M. Ivanovskaya, G. Branitsky, D. Orlik, et al., Nature of paramagnetic centres in tin dioxide, Russ. J. Inorg. Chem. 37 (5) (1992) 1147–1152.
[14] F.J. Berry, O. Helgasson, A. Bohorques, Preparation and characterization of tin-doped α-FeOOH (goethite), J. Mater. Sci. 10 (2000) 1643–1648.
[15] F.J. Berry, C. Greaves, O. Helgasson, et al., Synthesis and characterisation of tin-doped iron oxides, J. Mater. Chem. 9 (1999) 223–226.
[16] J. Kappler, N. Barsan, U. Weimar, Structure and reactivity of iron oxide surfaces, in: Proceedings of the International Conference on Eurosensors XI, vols. 3B1–3B3, Warsaw, Poland, 21–24 September 1997, p. 1177.
[17] P. Bogdanov, M. Ivanovskaya, E. Comini, et al., Effect of nickel ions on sensitivity of In_2O_3 thin film sensors to NO_2, Sens. Actuators B: Chem. 57 (1999) 153–158.
[18] M. Ivanovskaya, D. Kotsikau, D. Orlik, et al., About the possibility of metal oxide sensors application for environmental control, in: Proceedings of the International Workshop on New Developments on Sensors for Environmental Control, S. Cesarea Terme, Italy, 27–29 May 2002, p. 96.
[19] D. Kohl, Influence of water vapour on nanocrystalline SnO_2 to monitor CO and CH_4, Sens. Actuators B: Chem. 18 (1989) 71–113.
[20] J. Livage, J.P. Jolivet, E. Tronc, Electronic properties of mixed valence oxide gels, J. Non-Cryst. Solids 121 (1990) 35–39.
[21] G. Golodets, Catalysis Mechanism, Part 1, Nauka, Novosibirsk, 1984, p. 142.
[22] M. Ivanovskaya, D. Kotsikau, G. Faglia, et al., Influence of chemical composition and structural factors of Fe_2O_3/In_2O_3 sensors on their selectivity and sensitivity to ethanol, Sens. Actuators B: Chem. 96 (2003) 498–503.

Biographies

Dzmitry Kotsikau graduated from the Belarus State University in 2001 with honours; in the same year he entered the post graduate courses; simultaneously, he is working at the Scientific Research Institute for Physical and Chemical Problems of Belarus State University in the field of solid state chemistry and semiconductor gas sensors. His main scientific interests are Fe_2O_3–In_2O_3 and Fe_2O_3–SnO_2 nanosized composites, their structural and gas-sensitive characterisation.

Maria Ivanovskaya received her degree in chemistry in 1980 from Belarus State University in the field of photochemistry. Since 1989 she has been working at the Scientific Research Institute of Physical and Chemical Problems (Belarus State University). Her main scientific interest is solid state chemistry in applications to catalysis and semiconductor gas sensors, structural features of nanosized oxides (SnO_2, MoO_3, In_2O_3, Fe_2O_3) and oxide composites. She is co-author of more than 200 papers on the indicated topics.

Dmitry Orlik received his PhD degree in chemistry in 1990 from Belarus State University with a thesis on gas sensors and structural characterisation of oxide systems. Now he is occupying the research position in the Scientific Research Institute for Physical and Chemical Problems (Belarus State University). Now he is working in the field of solid state chemistry and semiconductor gas sensors.

Matteo Falasconi received an MS degree in physics with honours at University of Pavia in 2000, defending a thesis on non-linear surface optical properties of crystalline and porous silicon. From 2002 he is member of the Sensor Laboratory at University of Brescia as PhD student in materials engineering. He is involved in the study and characterization of semiconducting metal oxide sensors collaborating to the development of an electronic olfacting system.